Article:
Ravikumar, R., Thorpe, C.L. orcid.org/0000-0002-2860-8611, Corkhill, C.L. orcid.org/0000-0002-7488-3219 et al. (7 more authors) (2025) The effectiveness of TRIS and ammonium buffers in glass dissolution studies: a comparative analysis. npj Materials Degradation, 9 (1). 4. ISSN 2397-2106

https://doi.org/10.1038/s41529-025-00552-3

npj | materials degradation

Article

Published in partnership with CSCP and USTB

https://doi.org/10.1038/s41529-025-00552-3

The effectiveness of TRIS and ammonium buffers in glass dissolution studies: a comparative analysis

Ramya Ravikumar[1,2], Clare L. Thorpe[1] ✉, Claire L. Corkhill[3], Sam A. Walling[1], James J. Neeway[4], Carolyn I. Pearce[4], Albert A. Kruger[5], David S. Kosson[6], Jose Marcial[4] & Russell J. Hand[1]

Selecting appropriate buffers is crucial for evaluating the chemical durability of glass under controlled conditions such as in the EPA 1313 test designed to measure elemental release as a function of pH. The efficacy of two alkali-metal free buffers, TRIS ($NH_2C(CH_2OH)_3$) and ammonium chloride—ammonia (NH_3/NH_4Cl), was investigated during EPA 1313 testing of a simulated Hanford low-activity waste borosilicate glass in the alkaline regime (pH 8.5–10.5) at varying temperatures (RT, 40 °C, and 60 °C). While both buffers maintained the desired pH at room temperature, and up to 40 °C, the effectiveness of TRIS decreased at elevated temperatures, particularly at pH 10.5. Although ^{11}B NMR showed evidence of TRIS-B complexation, its effect on the rate of elemental release was found to be negligible under the test conditions. With ammonium buffer, the release of alkali cations was slightly elevated when compared to the same conditions with TRIS at early time points.

Glass dissolution tests are conducted with the following aims: (i) to assess the consistency of the glass product; (ii) to determine the relative durability of glasses; and (iii) to elucidate mechanisms controlling the glass dissolution rate. Various test methods include, but are not limited to, the product consistency test (PCT)[1], vapour hydration test (VHT)[2], single-pass flow-through test (SPFT)[3], and the pressurised unsaturated flow test (PUF)[4,5]. At the Hanford site, USA, all these tests have been performed on low-activity waste (LAW) glass compositions[6,7] that will be used to immobilize radioactive waste at the waste treatment and immobilization plant (WTP). Though each of the aforementioned tests helps improve understanding of glass behaviour, only the PCT and VHT are currently used to assess glass durability as part of the established WTP operations contract[8]. Once produced, the LAW glasses will be disposed of in the near-surface, integrated disposal facility (IDF) at the Hanford site. Recently, the glass leaching assessment for disposability (GLAD) project has evaluated the use of established U.S. Environmental Protection Agency (EPA) test methods, as alternatives to the PCT and VHT to assess the short-term chemical durability of LAW glasses[9,10]. The EPA 1313 methodology was designed to study the effects of pH on elemental release from a material over a short experimental duration. The test has been modified slightly for use on nuclear waste-type glass (primarily the specification of a particle size range) to measure elemental release over a pH range and temperature more relevant to those expected in the IDF[9,11].

In many dissolution tests, including the EPA 1313, maintaining a constant pH is desirable if the test is being used to measure the response of material under constrained conditions, for example, to obtain pH and temperature-dependent kinetic data or to simulate real subsurface disposal conditions where some buffering capacity exists[12]. In general, glass corrosion brings about a change in solution chemistry due initially to glass surface dealkalization while the glass contacts an aqueous solution. As a result, the pH of the solution increases and catalyses the hydrolysis of network bonds, thereby increasing the glass dissolution rate[13]. An increase in pH will also affect the solubility of aqueous species and the formation of secondary mineral phases. Tests like the EPA 1313 aim to measure the elemental release as a function of pH[5]; however, as the pH in the EPA 1313 test conducted on glass varies throughout the test it is not possible to explicitly quantify the impact of a particular pH on durability. One method of stabilizing the pH is by using a chemical buffer, but the choice of buffer should be such that it does not affect the glass dissolution rate and should cover the alkaline regime relevant to many radioactive waste glass disposal conditions[14]. The pH of groundwater in the IDF is mildly alkaline (pH ~ 8) and is likely to increase in the immediate vicinity of the waste due to the interaction of groundwater with cementitious material and with the glass itself[15]. Buffers containing sodium and its salts, such as sodium phosphate and sodium carbonate-bicarbonate, should be avoided to prevent any

[1]School of Chemical, Materials and Biological Engineering, University of Sheffield, Sheffield, UK. [2] Department of Chemistry, BMS Engineering College, Bengaluru, India. [3]School of Earth Sciences, University of Bristol, Bristol, UK. [4]Pacific Northwest National Laboratory, Richland, WA, USA. [5]Office of River Protection, U.S. Department of Energy, Richland, WA, USA. [6]Department of Civil and Environmental Engineering, Vanderbilt University and CRESP Nashville, Nashville, TN, USA. ✉e-mail: clare.thorpe@sheffield.ac.uk

impact on glass corrosion behaviour, as sodium is a constituent of the nuclear waste glass matrix[5]. Metal chlorides/hydroxides such as LiCl/LiOH and KCl/KOH (which maintain a constant pH) have also been shown to alter the glass dissolution rates[5,16] by affecting the ion exchange equilibrium, while the counter anion (Cl^-) has a negligible effect[17]. Therefore, it is preferable to use metal-free buffers to avoid any influence on the dissolution mechanism.

Organic buffers can be a suitable choice in this regard, and a variety have been considered for glass dissolution experiments in the pH range of 6.8–11.4[18,19] (Supplementary Fig. 1). It is worth noting that organic buffers that require the use of metal-containing bases such as NaOH or KOH to adjust the pH to the desired range cannot be considered metal free. Tris(hydroxymethyl)aminomethane, also known as TRIS, buffer ($NH_2C(CH_2OH)_3$, is one example of a cationic organic buffer that offers the advantage of achieving the desired pH range through the addition of acids such as HCl or HNO_3. It has a pK_a value of 8.3 at 25 °C, making it suitable for maintaining a stable pH within an effective range generally reported between pH 7–9[20]. TRIS buffers have been commonly used in glass dissolution studies[7,21], but concerns have been raised regarding the formation of TRIS-boron complexes (TRIS boric and/or TRIS borate) in the alkaline regime when using the buffer in experiments with borosilicate glass (the majority of nuclear waste glass are borosilicates). Boron is both a network former and commonly used as a tracer for dissolution as it is not normally retained in alteration layers, therefore, it is important to understand the potential impact of the TRIS boric/ TRIS borate complex on measured glass dissolution rates[22,23].

TRIS-boron complex formation depends on several parameters including the composition of the glass, pH and temperature conditions, the acid used (HNO_3/HCl), and the ratio of TRIS/acid and $B(OH)_3$ in solution[22]. Boric acid [$B(OH)_3$], a Lewis acid that remains prevalent at neutral pH with a pK_a value of 9.24, is released into solution upon hydrolysis of terminal boron-oxygen bonds in the borosilicate glass network. Boric acid forms a tetrahedral borate anion $\left[B(OH)_4^-\right]$ that becomes the dominant boron species in more basic conditions[24]. There remains uncertainty whether the formation of TRIS-boron complexes can affect the glass dissolution rate and, thus, the boron release rate from the glass[22,23].

The present study compares the efficacy of TRIS buffer with ammonium buffer, NH_3/NH_4Cl, which is a metal-free inorganic buffer with a $pK_a = 9.25$ at 25 °C. Ammonium buffer is the combination of a weak base (NH_3) and its salt NH_4Cl (conjugate acid NH_4^+)[25]. The effective pH range of ammonium buffer lies between 8.24 and 10.24 at 25 °C[26]. Although ammonium buffer has been used in durability tests on ceramic systems[27] and glasses[28], there are no reports to date regarding the potential for solution complex formation during glass dissolution tests.

Using the EPA 1313 test protocol, the current work first evaluates the use of TRIS and ammonium buffers with LAW-type borosilicate glass (known as LAWA44)[29] under a range of buffer concentrations and temperatures. Secondly, the impacts of pH and temperature on glass dissolution in these buffered systems are studied to derive dissolution rate data and a mechanistic understanding of glass corrosion from the EPA 1313 test response.

Results

Glass dissolution is pH dependent, and the dissolution of many borosilicate glasses, including LAWA44, causes a shift in pH to more alkaline values[5]. An unbuffered EPA 1313 dissolution test was first performed to demonstrate the extent of this pH drift at low temperatures and short timescales. The test followed the scheme outlined in Fig. 1 at room temperature (RT) using LAWA44 glass and ASTM Type 1 water (defined as having a resistivity of >18 MΩ-cm, a conductivity of <0.056 μS/cm and <50 ppb of total organic carbon)[30].

Over 192 h, without any buffer, a change in pH from 7.45 (recorded after the glass powder) to 10.04 was measured in the Type 1 water system and attributed to ion exchange processes as observed by the higher release of Na (Fig. 2). The normalised mass loss (NL_i) for all the elements in a system buffered to pH 8.5 ± 0.1 (the approximate midpoint of the pH range experienced in the unbuffered Type 1 water system) by 0.1 M TRIS/HNO_3 was somewhat lower when compared to unbuffered NL_i values (Fig. 2) since the pH in buffered tests is maintained and does not increase as the glass dissolves. This comparison highlights the importance of pH control on elemental release data.

TRIS buffer

Effect of TRIS buffer concentration. Since buffering capacity depends on the concentration of the buffer used[22], systematic investigations were carried out to understand the pH stability of TRIS buffer at an optimal buffering concentration. This concentration was determined by conducting a series of EPA 1313 experiments at room temperature at a target pH of 8.5, and monitoring the pH deviation as a function of time at four different concentrations of TRIS (0.02 M, 0.05 M, 0.1 M, and 0.3 M). The normalised mass loss (NL_i) of key elements from the glass at each concentration was also measured. For all of the TRIS concentrations, a

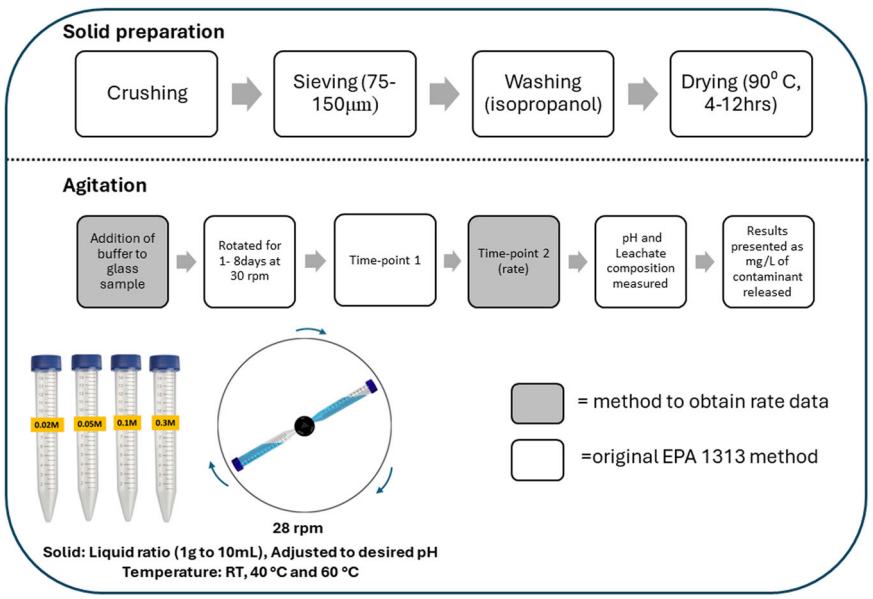

Fig. 1 | EPA 1313 test method. Schematic representation of EPA 1313 protocol adapted from EPA, 2017.

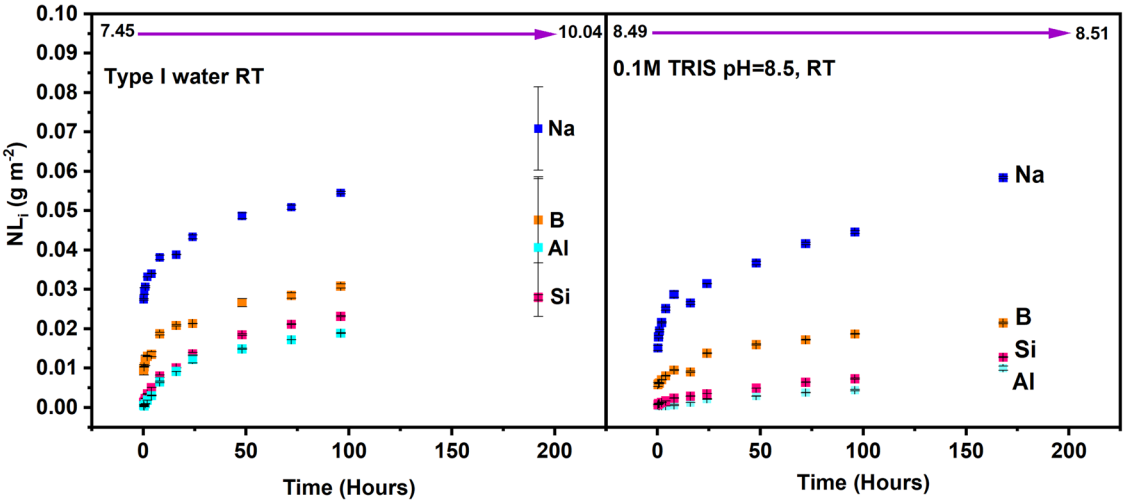

Fig. 2 | NL_i as a function of time for LAWA44 glass in Type I water (left) and 0.1 M TRIS–HNO_3, pH 8.5 (right) at RT. Error bars represent one standard deviation of triplicate measurements, where error bars are not visible they are smaller than the symbol size.

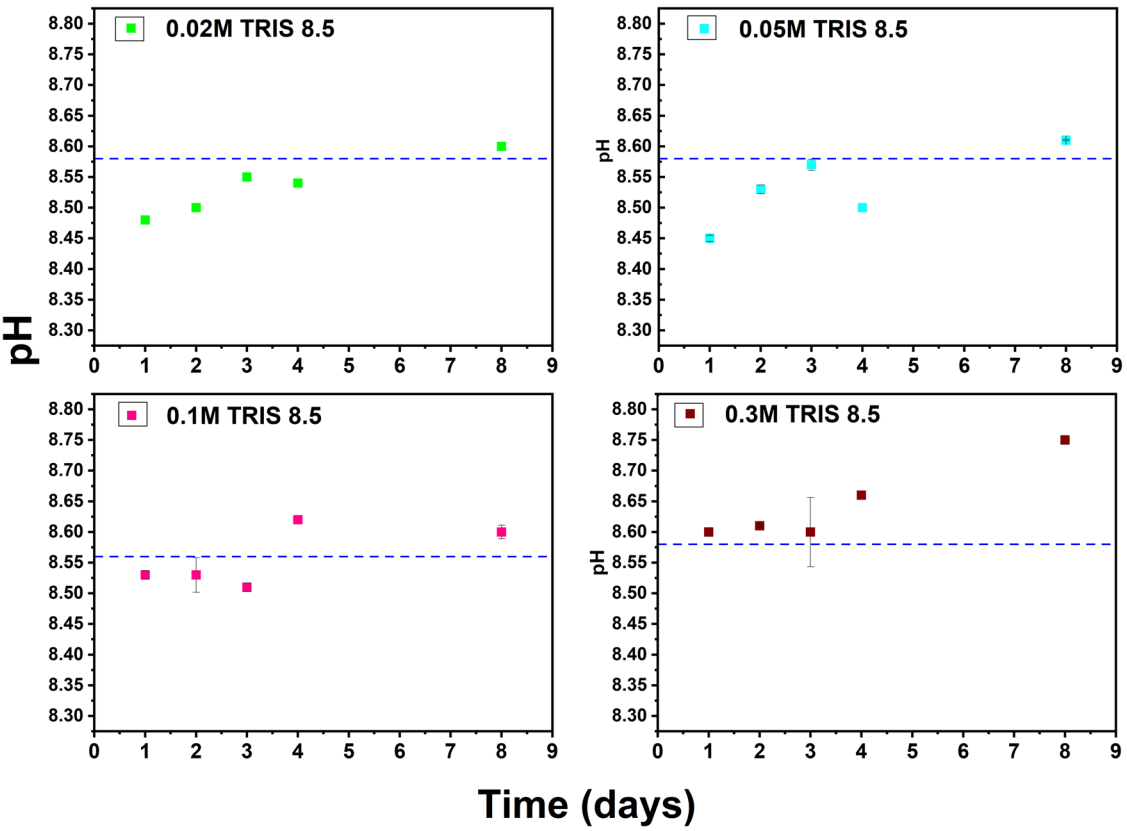

Fig. 3 | pH as a function of time for varying concentrations of TRIS buffered media. Glass was added to solution buffered with 0.02, 0.05, 0.1 and 0.3 M TRIS at RT and a target pH of 8.5 (the ▪▪▪▪▪ set pH value is represented by the blue dashed line).

similar trend in the normalised elemental mass loss of Na > B > Si > Al was observed with the only difference being slightly lower Na and B release at 0.3 M TRIS (Supplementary Fig. 2 and Supplementary Tables 1 and 2). NL_B was $(1.92 \pm 0.06) \times 10^{-2}$ g m^{-2}, $(1.87 \pm 0.06) \times 10^{-2}$ g m^{-2}, $(1.81 \pm 0.01) \times 10^{-2}$ g m^{-2} and $(1.67 \pm 0.01) \times 10^{-2}$ g m^{-2} for 0.02, 0.05, 0.1, and 0.3 M TRIS buffer respectively after 4 days (Supplementary Table 2).

With the increase in TRIS concentration from 0.02 M to 0.1 M, the pH deviation was reduced, indicating an improvement in the buffering capacity. Figure 3 depicts the change in pH from the set pH values after adding glass to different concentrations of buffer solutions. Here the 'set pH' was the pH measured at the start of the experiment and was always within 0.1 of the target pH; for example, for a target pH of 8.5, an acceptable set pH was between 8.41 and 8.59. All solutions show minimal deviation from the set pH (< 0.3 pH units), however, the solution with 0.1 M TRIS/HNO_3 buffer showed the lowest deviation (pH = 8.51–8.62) from the set pH value of 8.56 throughout the experimental duration (1–8 d) when compared to other concentrations (0.02, 0.05, and 0.3 M). This conclusion is further substantiated by determining the average pH during the 8-day duration, which remains closest to the set value (8.56) for 0.1 M TRIS/HNO_3 buffered

solution (Supplementary Table 3), and the observation that, although very slight, a decrease in NL_i was observed in the 0.3 M TRIS buffer experiment when compared to the 0.02 M, 0.05 M, and 0.1 M experiments (Supplementary Table 2). Similar findings were reported for short-term experiments (24 h) with a three-oxide glass where 0.1 M was concluded to be an effective concentration for glass systems[22]. Based on these observations, a concentration of 0.1 M TRIS was selected for further studies.

TRIS buffering capacity

Once it was determined that 0.1 M TRIS could maintain a stable pH over the desired experimental duration at RT, experiments were performed at temperatures of RT, 40 °C and 60 °C with target pH values of 8.5, 9.5, and 10.5 (all pH values measured at RT) to investigate the ability of 0.1 M TRIS solutions in contact with LAWA44 to maintain a constant pH at more alkaline regimes. The TRIS buffer demonstrated effectiveness at all tested pH values at RT (Supplementary Fig. 3), exhibiting minimal variation in the measured pH over 8 days compared to the blank solution containing only TRIS (denoted as a red * in Supplementary Fig. 3).

At 40 °C, the pH values showed a slight increase from the desired pH value (+0.2 pH units) during the initial time points (up to 20 h) (Supplementary Fig. 3), after which they remained stable at the set pH values ± 0.1 throughout the experimental duration of 192 h for target pH values of 8.5 and 9.5. However, at target pH 10.5, the pH dropped by 0.5 pH units between 48 h and 96 h and remained at that pH until the end of the experiment. The pH was maintained within ±0.5 pH units even at 40 °C. When measuring the pH change for a blank TRIS buffer and TRIS with glass at 40 °C, a pH reduction from 10.5 to 10.1 was observed for both solutions (Supplementary Fig. 3) indicating that this change may be attributed to the temperature-dependent pK_a of the TRIS buffer, that would decrease from 8.30 at 20 °C to 7.68 at 40 °C[31]. These experiments were conducted in air and so the solution equilibrium with regard to CO_2 must be considered. Dissolution of CO_2 into solution, and associated formation of carbonic acid, is expected under all conditions, however, at the high pH of 10.5, combined with TRIS's reduced buffering capacity at elevated temperatures, the solution appears more susceptible to pH changes due to CO_2 absorption.

At 60 °C, the set pH was maintained ±0.1 for both the 8.5 and 9.5 experiments after a temporary increase of 0.2 and 0.3 pH units in the initial 24 h. However, for the target pH of 10.5, the blank buffer solution showed a drift from 10.55 (at 15 min) to 10.11 (at 168 h) (Supplementary Fig. 3), whilst in tests containing glass, the pH value reduced significantly from 10.52 (15 min) to 8.94 (168 h). At 60 °C the pK_a of TRIS would be 7.06 and this may explain the reduction in buffering capacity over time especially given that pH 10.5 is slightly outside the buffering range of TRIS (pK_a = 8.3)[32]. This study confirms that the TRIS can be used to maintain a stable pH in these types of glass dissolution experiments between pH 7.0–10.5 for up to 40 °C and between pH 7.0–9.5 for 60 °C for the specific test conditions and timeframe of the EPA 1313 test studied here (8 days; standard EPA 1313 test 48 h). It is likely that the fact that glass dissolution tends to increase solution pH helps in maintaining pH 9.5 and 10.5 at higher temperatures despite the reduction in TRIS pKa.

Effect of temperature and pH on elemental release in TRIS buffer media. The normalised mass loss (NL_i) for Na, Si, Al and B were calculated for the different pH and temperatures investigated (Supplementary Tables 4–7). Regardless of the conditions, sodium (NL_{Na}) was released faster than the other elements, as illustrated in Fig. 4. This finding

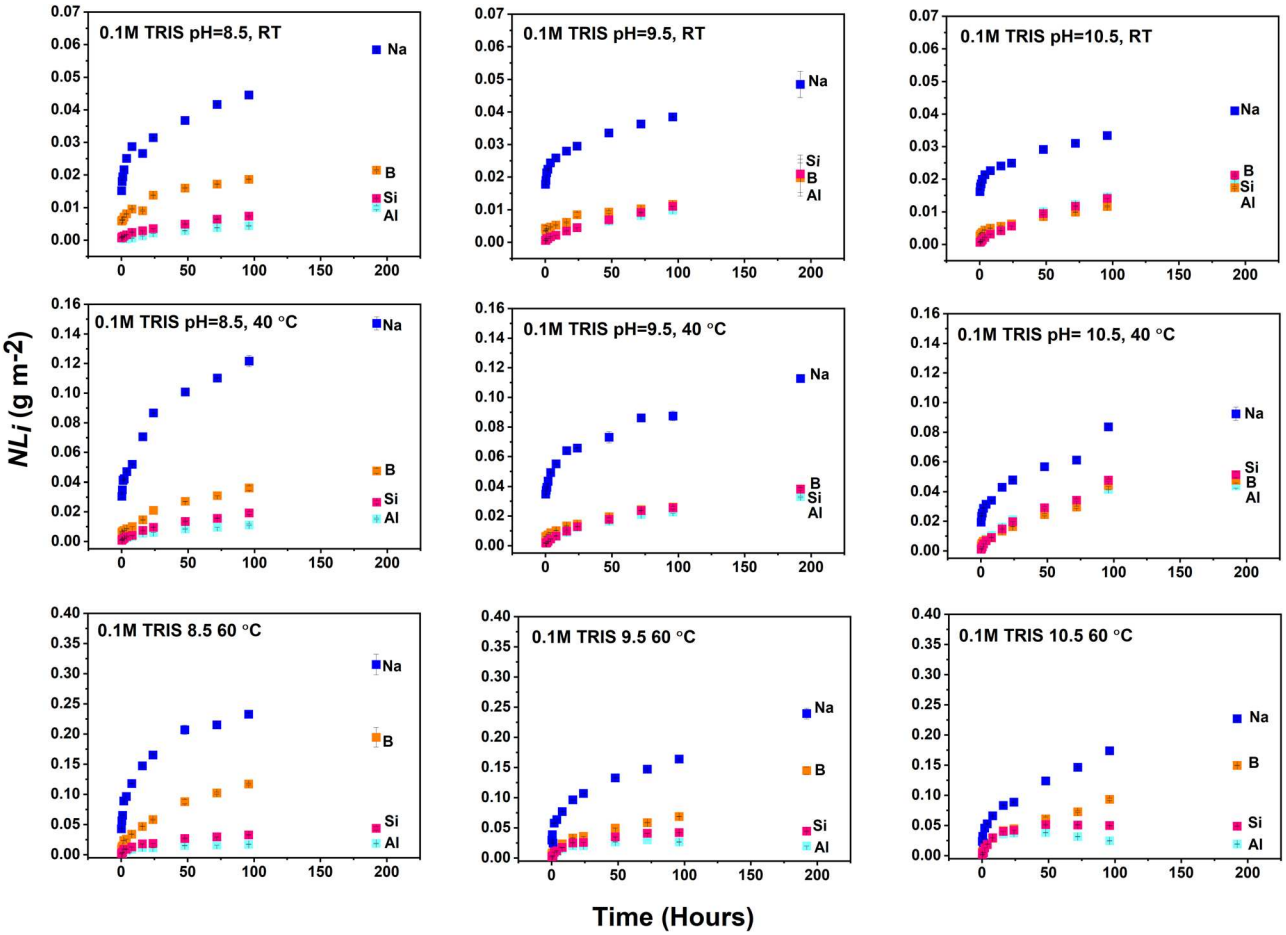

Fig. 4 | NL_i (Na, B, Si, and Al) as a function of time for LAWA44 glass at target pH = 8.5, 9.5, and 10.5 of 0.1 M TRIS–HNO_3 solution at RT, 40 °C, and 60 °C. Error bars represent one standard deviation of triplicate measurements, where error bars are not visible they are smaller than the symbol size.

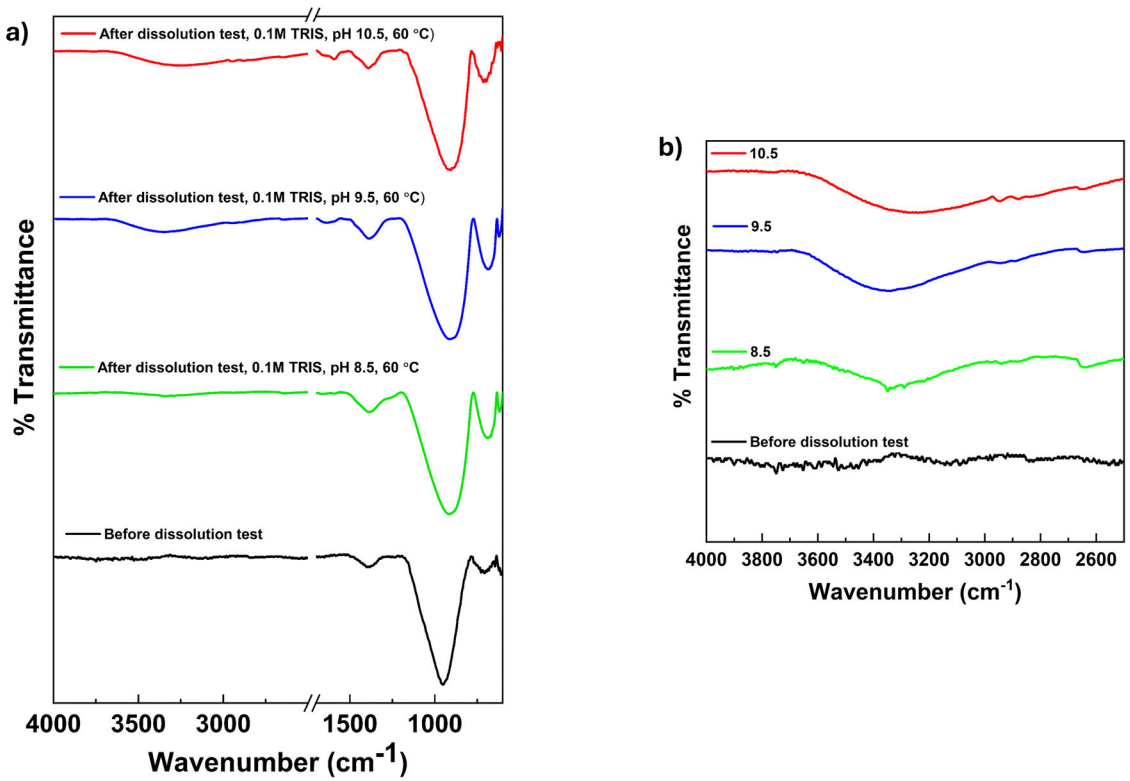

Fig. 5 | FT-IR spectra of LAWA44 before and after dissolution. a FT-IR spectra of day 8 sample in pH 8.5, 9.5 and 10.5 of 0.1 M Tris–HNO_3 solution at 60 °C. **b** Enlarged view of the –OH stretching region.

aligns with previous studies that suggest the combined influence of ion exchange and matrix dissolution on the release of alkali elements[22,33,34]. It is also important to note that at RT, with an increase in target pH from 8.5 to 10.5, there was a gradual decrease in the sodium release (Fig. 4), consistent with a reduced influence from ion exchange (driven by H_3O^+ concentration) with increasing pH. Meanwhile, the NL_i values for Si and Al slightly increased with increasing pH, eventually becoming congruent with B at higher pH.

At 40 °C, the NL_i values for all elements were approximately twice those of the room temperature results (Fig. 4). Similar to the data collected at RT, an increase in the target pH, from 8.5 to 10.5, resulted in a reduction in the release of sodium, while B, Si and Al tended to attain congruency.

At 60 °C, the NL_i values increased fourfold when compared to those obtained at RT (Fig. 4). The release of Na, B, Si, and Al increased with time at target pH 8.5; however, at pH 9.5 and 10.5, the release of Al and Si reduced between 48 h and 72 h. The incongruent release of Si and Al under most test conditions is indicative of the formation of a gel layer[35]. Post-dissolution powder XRD evidenced no crystalline phases within the limits of detection (Supplementary Fig. 4). However, FT-IR analysis (Fig. 5) of samples post-dissolution, showed a characteristic IR vibration at 3298 cm^{-1} and 950–1150 cm^{-1} confirming the presence of molecular water, Si–OH, Al–OH and B–OH hydrogen bonding at the surface of the glass[36].

NMR characterization of boron species in reference solutions. To investigate the presence of the TRIS-boron complex,^{11}B NMR experiments at the three target pH values (8.5, 9.5, and 10.5) and temperature (RT, 40 °C, and 60 °C) conditions were performed and compared to reference solutions; all pH values were measured at RT. Spectra were acquired with 10% H_2O/D_2O as the solvent for both samples and reference solutions. Initially, ^{11}B NMR data were collected for reference boron species (boric acid) to verify the instrumental parameters. These results showed a sharp peak at 19.02 ppm for pH 7.5 at RT (Supplementary Fig. 5), similar to chemical shift values obtained by Stone-Weiss et al.[22]. and within ±3 ppm of the chemical shift for boric acid at pH 7.5 reported by Tournié et al.[23]. With the increase in pH to 8.5, 9.5, and 10.5, the chemical shift gradually moved to up-field values of 16.37 ppm, 7.51 ppm, and 2.94 ppm confirming the presence of $\left[B(OH)_4^-\right]$ species (Supplementary Fig. 5). A 1:1 mixture of 0.1 M TRIS/B solution at RT showed two distinct peaks, one corresponding to the boric acid/borate species and the other to TRIS-B complexes (Supplementary Fig. 6). At pH 8.5, the chemical shift value of 17.52 ppm corresponds to boric acid. This peak gradually shifted to 8.94 ppm at $pH_{(RT)}$ 9.5 and 3.22 ppm at pH 10.5 indicating the formation of $\left[B(OH)_4^-\right]$ with increasing pH. Two additional peaks at 1.14 ppm and 0.56 ppm for pH 8.5, 1.04; and 0.51 ppm for pH 9.5, and 1.00 ppm and 0.49 ppm for pH 10.5 correspond to TRIS-boric and TRIS-borate complexes, respectively (Supplementary Fig. 6). With an increase in pH there are consistent shifts of these peaks to up-field values indicating the co-existence of boric/borate species along with the TRIS complexes.

To understand complex formation at elevated temperatures, in-situ heated ^{11}B NMR were recorded for a 1:1 mixture of a TRIS/B solution (Supplementary Figs. 7 and 8). At 40 °C and pH 8.5, the peak with a chemical shift of 18.15 ppm was attributed to boric acid and the peak at 1.44 ppm was attributed to TRIS-boric complex (Supplementary Fig. 7). At 40 °C and pH 9.5, there was a gradual shift of the boric acid peak to 10.34 ppm and of the TRIS-boric species to 1.24 ppm (Supplementary Fig. 7). The intensity of the boric acid peak decreased while the peak corresponding to the TRIS/B complex increased demonstrating the prevalence of the latter complex at high temperature. At the slightly more alkaline pH of 10.5, the peak shifted to an up-field value of 4.50 ppm, which corresponds to the borate species. Two sharp peaks at 1.19 ppm and 0.70 ppm confirmed the presence of two TRIS/B complexes (Supplementary Fig. 7). Again, the intensity of borate species became weaker and sharp peaks are observed for TRIS/B complexes with an increase in pH. Similar results were obtained for 60 °C with increasing pH from 8.5 to 10.5 (Supplementary Fig. 8). When considering how solutions of the same pH vary with temperature, the intensity of the TRIS/B complex decreases in intensity when compared to the borate/boric acid species with increasing temperature implying more of

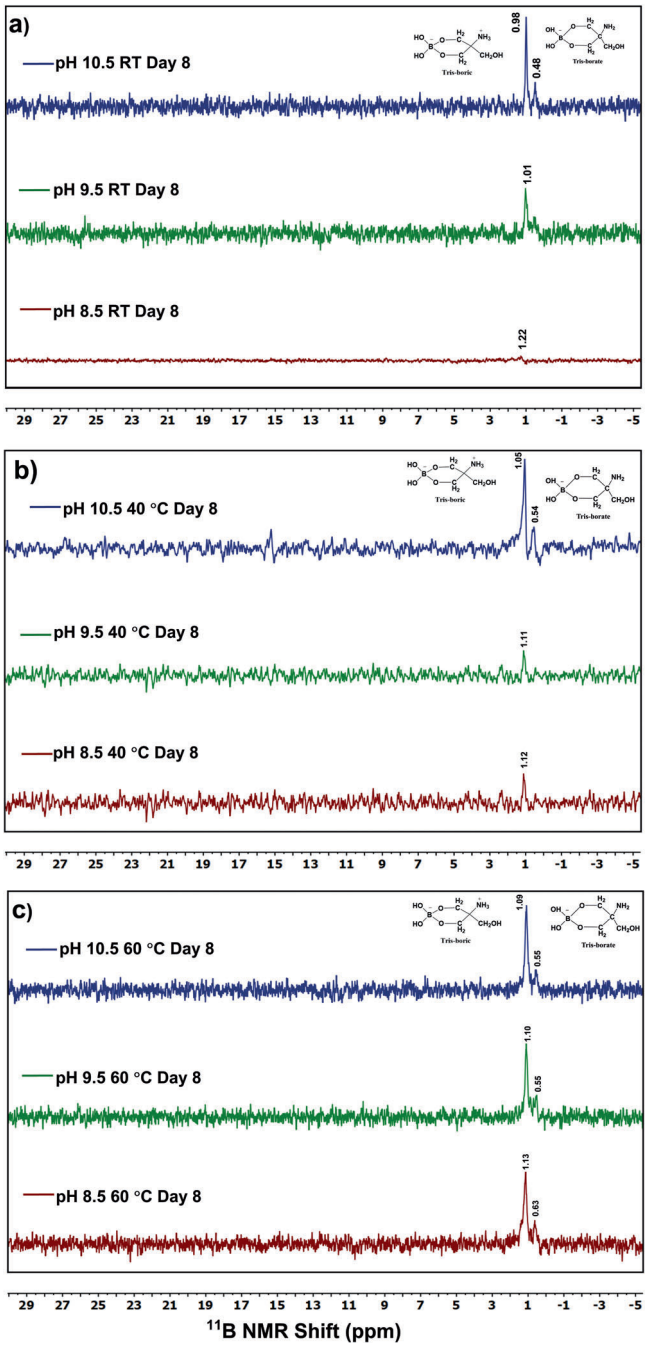

Fig. 6 | ^{11}B NMR spectra of the aliquot leachate collected on day 8 of dissolution experiments at. a RT, **b** 40 °C, and **c** 60 °C with set pH of buffered at 8.5, 9.5, and 10.5 with TRIS.

the boron is present as TRIS/B at lower temperatures (Supplementary Figs. 6–8).

NMR characterization of boron species after leaching experiments. Aqueous samples from the EPA 1313 method collected post-dissolution on day 8 at RT exhibited a chemical shift value of 1.22 (minor peak) and 1.01 ppm at pH 8.5 and 9.5, respectively, corresponding to TRIS-boric complex (Fig. 6). Meanwhile, at pH 10.5, two distinct peaks at 0.98 ppm and 0.48 ppm were observed, attributed to the presence of TRIS-boric and the TRIS-Borate complexes, respectively (Fig. 6).

Similarly, at 40 °C, the presence of the TRIS-boric complex was observed at lower pH (pH 8.5 and 9.5) and both complexes (TRIS-boric and TRIS-borate) were observed at higher pH (pH 10.5) (Fig. 6). Whereas at 60 °C, irrespective of the pH conditions, both TRIS complexes were observed possibly as concentrations of boron in solution increased with increased reaction progress at higher temperatures making the detection of boron species above experimental noise easier. The results from the as-prepared 1:1 TRIS boron reference solution (Supplementary Figs. 6–8) show the coexistence of TRIS complexes with boric acid (at low pH levels) and borate anion (at high pH levels) even at RT. In contrast, the boric acid and borate anion peaks are absent from sample NMR spectra. The absence of boric acid or borate anion in the aliquot samples likely reflects the temperature dependence of the TRIS-B complex (that can be seen to dominate at lower temperatures in the standards) and the lower concentration of boron in sample aliquots compared to the standards meaning that the boric acid and borate anion peaks may be below the limit of detection in samples.

Although TRIS-boron complexation was observed, the effect of these complexes on the glass dissolution rate cannot be determined by studying the TRIS-buffer system alone and therefore the EPA 1313 test response for LAWA44 glass was probed with the ammonium buffer, a buffer that was not expected to complex with boron.

Ammonium buffer

Optimization of ammonium buffer concentration. The same dissolution tests were performed using ammonium buffer (NH_3/NH_4Cl) to compare with results from the TRIS buffer. The optimal concentration for kinetic studies was investigated in a similar manner: with 8-day modified EPA 1313 tests.

Regardless of the ammonium buffer concentration used, the normalised release was in the order Na > B > Si > Al (Supplementary Fig. 9) and similar to the experiments in TRIS. At concentrations of 0.02, 0.05, and 0.01 M pH was maintained within 0.3 units of the set value whilst for concentrations of 0.3 M the pH was maintained at 0.4 units of the set value over 8 days (Fig. 7 and Supplementary Tables 8–10).

The only notable difference was a slight increase in the NL_{Na} with increasing concentration, for example, in the initial 24 h the NL_{Na} was $(2.34 \pm 0.00) \times 10^{-2}$ g m^{-2}, $(4.59 \pm 0.15) \times 10^{-2}$ g m^{-2}, $(5.15 \pm 0.11) \times 10^{-2}$ g m^{-2} and $(7.28 \pm 0.17) \times 10^{-2}$ g m^{-2} and after 48 h NL_{Na} was $(5.36 \pm 0.00) \times 10^{-2}$ g m^{-2}, $(5.36 \pm 0.08) \times 10^{-2}$ g m^{-2}, $(5.70 \pm 0.01) \times 10^{-2}$ g m^{-2} and $(6.89 \pm 0.15) \times 10^{-2}$ g m^{-2} for glass leached in solutions of 0.02 M, 0.05 M, 0.1 M, and 0.3 M ammonium buffer respectively (Supplementary Tables 8 and 9). Boron, silicon and aluminium releases were similar across the different concentrations with a slight decrease in NL_i observed at 0.3 M. It is possible that, despite its larger ionic radius, NH_4^+ (1.40–1.67 Å)[37,38] may contribute to ion exchange processes with Na^+ (0.99–1.39 Å)[37,38] and thus may induce the release of sodium from the glass surface with effects more pronounced at higher ammonium concentrations. Ammonium ion exchange for sodium has been studied for ion exchange resins, clays, phosphates, and zeolites[39–41] but little is known about interactions with glass, it is highly unlikely that NH_4^+ can penetrate into the glass but surface effects cannot be ruled out. A concentration of 0.1 M ammonium buffer was chosen for further experiments at target pH 8.5, 9.5 and 10.5 with different temperatures (RT, 40 °C and 60 °C) as it showed good buffering capacity and normalized mass loss values comparable with those obtained with the TRIS buffer at the same concentration.

Ammonium buffering capacity

As with the TRIS buffer, the pH was set within 0.1 of the target pH. At all temperatures, when glass was added to the buffer solution, the pH was maintained within 0.3 of the set pH with the exception of the 60 °C system at a target pH of 8.5 (Supplementary Fig. 10). In this experiment the pH increased from 8.5 to 9.0, a deviation which was not observed in solutions with target pH values of 9.5 and 10.5. This is a minimal deviation when compared to that observed with Type I water with glass, which showed the pH increase from near-neutral to 10.23 and 10.34 for 40 °C and 60 °C, respectively (Supplementary Fig. 11). Hence, the ammonium buffer was

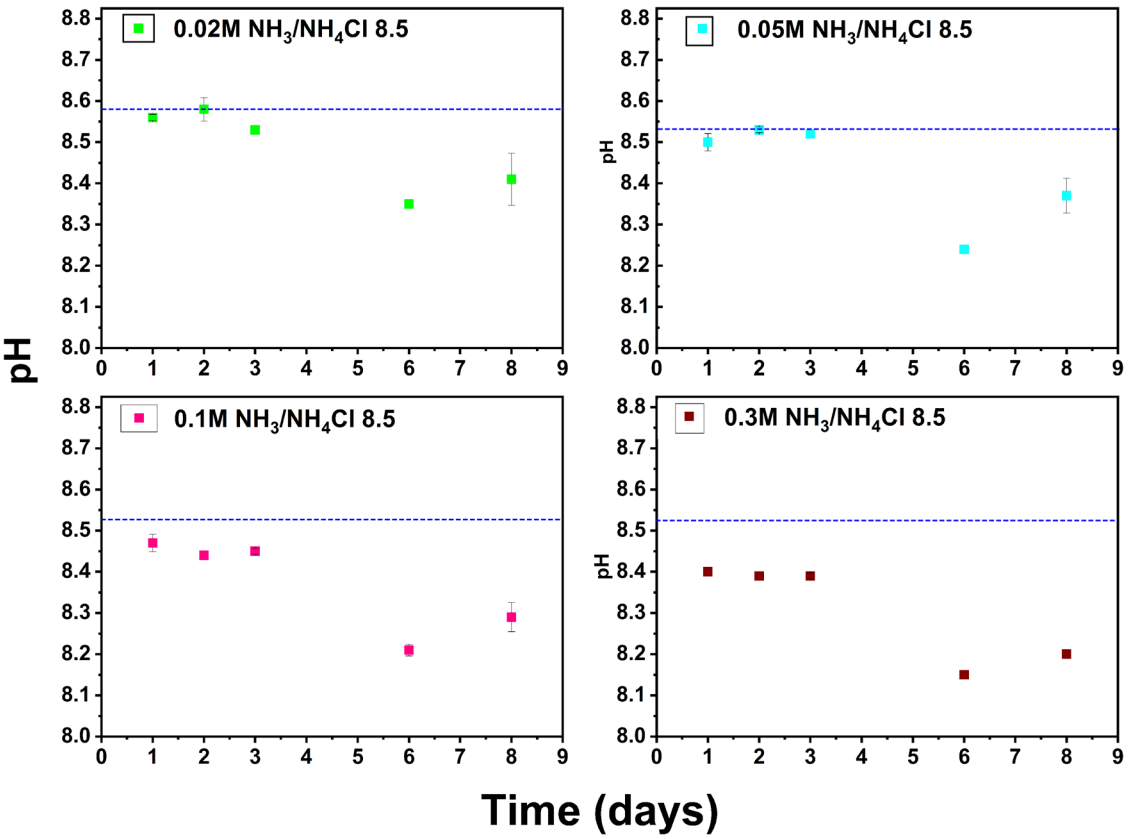

Fig. 7 | pH as a function of time for varying concentrations of NH_3/NH_4Cl buffered media. Glass was added to solution buffered with 0.02, 0.05, 0.1 and 0.3 M NH_3/NH_4Cl at RT and a target pH of 8.5 (the ▪▪▪▪▪ set pH value is represented by the blue dashed line).

effective at specific pH target values, with the ideal buffering range lies between 8.25 and 10.25 (RT).

Effect of temperature and pH on elemental release in ammonium buffer media and comparison with TRIS buffer media. When comparing elemental release values for the equivalent temperature and pH conditions with TRIS buffer the results were similar, although NL_i (particularly sodium) were slightly higher in the ammonium buffer at higher temperatures when compared to TRIS buffer (Figs. 4 and 8 and Supplementary Tables 11–14). This observation supports the theory that NH_4^+ is participating in ion exchange with Na^+ at the glass surface. As observed with TRIS buffer, NL_{Na} was twice the value of NL_B, and the sodium release decreased with an increase in target pH from 8.5 to 9.5 at RT (Fig. 8). NL_B and NL_{Si}, in contrast, remained at similar values across the pH range for both buffers at RT (Figs. 4 and 8) with boron values slightly elevated in ammonium buffer compared to TRIS.

The ammonium buffer exhibited incongruent leaching of B, Si and Al at RT, 40 °C and 60 °C under high pH conditions (9.5 and 10.5) (Fig. 8), which is in contrast to the congruency observed with TRIS buffer. For instance, in ammonium buffer at 40 °C and target pH 9.5, after 8 days the NL_B was $(6.72 \pm 0.26) \times 10^{-2}$ g m^{-2}, slightly higher than for NL_{Si} ($(4.13 \pm 0.35) \times 10^{-2}$ g m^{-2}) and NL_{Al} ($(2.90 \pm 0.36) \times 10^{-2}$ g m^{-2}); compared to $NL_B = (3.85 \pm 0.08) \times 10^{-2}$ g m^{-2}, $NL_{Si} = (3.83 \pm 0.09) \times 10^{-2}$ g m^{-2} and $NL_{Al} = (3.30 \pm 0.04) \times 10^{-2}$ g m^{-2} in TRIS buffer under the same temperature and pH conditions. It is notable that NL_{Si} and NL_{Al} were comparable in both buffered media; however, the difference resides in the release of B, which is higher than Si and Al in all of the ammonium buffered media under all conditions except pH 10.5 at RT.

At 60 °C, the elemental releases at 8 days almost doubled when compared with those obtained at 40 °C (Fig. 8). NL_{Na} and NL_B were comparable to the same conditions in the TRIS buffered system except at pH 10.5 where release rates in TRIS buffer were higher. This is likely due to the difficulty in maintaining pH 10.5 in the TRIS buffered system and the subsequent reduction in pH observed that would favour increased ion exchange.

^{11}B NMR investigations were performed on aqueous solutions sampled after 8 days of leaching in ammonium-buffered solutions at RT under pH 8.5, 9.5, and 10.5. No signals indicative of ammonia-boron complexes were observed (Supplementary Fig. 12) confirming that boron does not interact with ammonia to form detectable complexes under these conditions. Signals related to boron (boric acid and borate) were absent suggesting that boron concentration in these aliquots may be below the limit of detection or not be present as the detectable ^{11}B isotope. It is worth noting that, while detectable TRIS-B complexes were observed in TRIS buffered systems with glass, neither boric-acid or borate were observed in day 8 samples (in contrast, a 1:1 mixture of TRIS and boric acid prepared as a reference solution exhibited signals corresponding to boric acid and borate). While the reason remains unclear, the concentrations of boron in each system were similar, and so both are likely below the detection limit for boric acid/borate at RT; similar limitations in ^{11}B NMR detection have been reported[21].

Glass dissolution rate and activation energy

Two different trends in the release of elements during initial and later time points of the EPA 1313 test protocol were observed, and therefore, two sets of time points are considered to determine the associated normalized dissolution rate for boron (NLR_B) (Table 1). First, an early rate between 15 min and 8 h, and second a later rate between 24 h and 96 h (the 192 h (8 d) timepoint sometimes deviated from the linear trend). Finally, an average rate across the complete time period from 15 min to 8 d was also calculated.

The results show a faster dissolution rate of boron during the early time periods 15 min–8 h of up to an order of magnitude higher than the rate measured between 24 h and 96 h; for example, at RT and target pH 8.5 for the TRIS buffer system, the measured rate decreased from $(4.74 \pm 0.34) \times 10^{-4}$ g m^{-2} d^{-1} (15 mins–8 h) to $(6.62 \pm 0.60) \times 10^{-5}$ g m^{-2} d^{-1} (24 –96 h) (Table 1). As expected, NLR_B increased with temperature; for

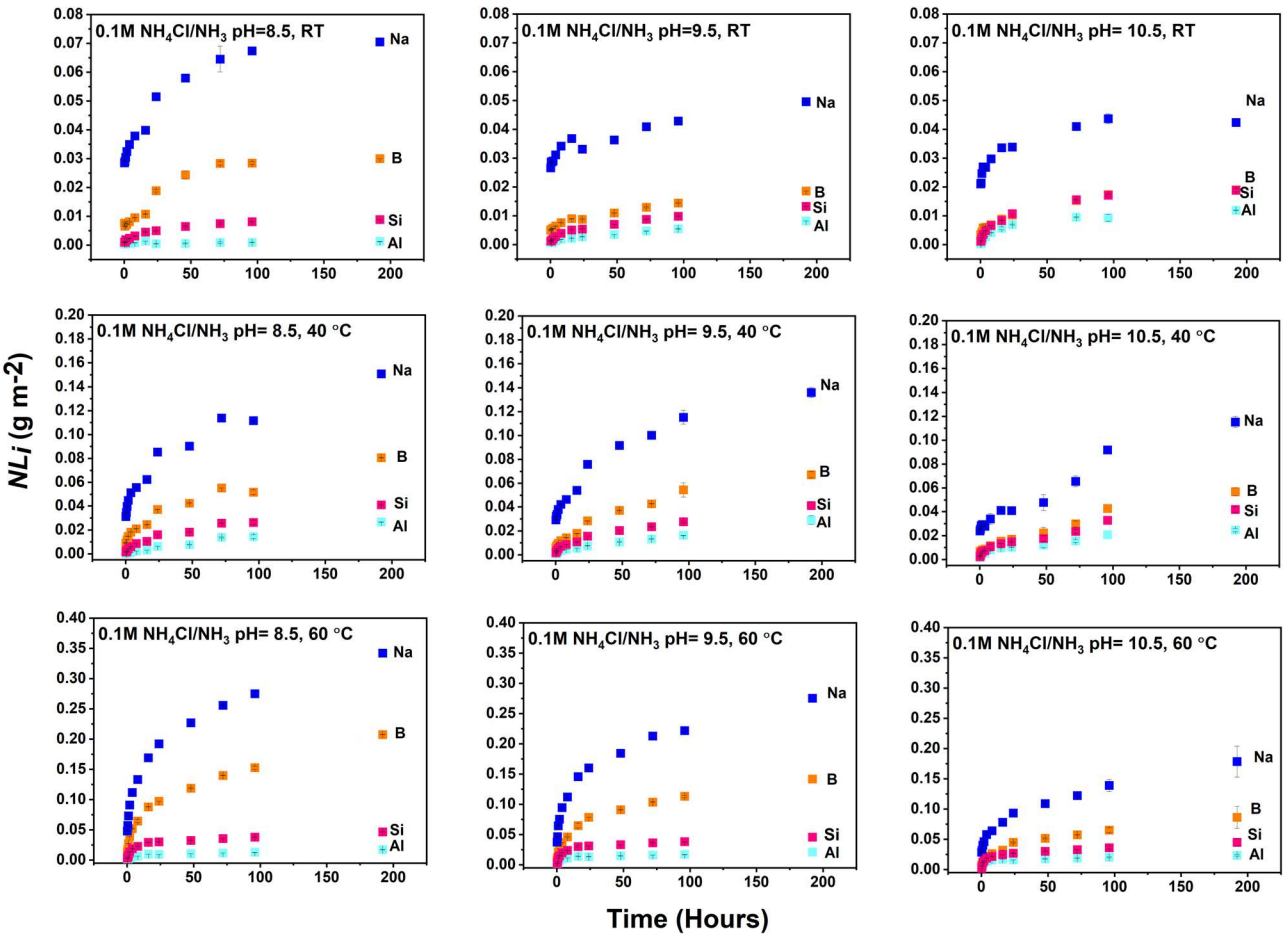

Fig. 8 | NL_i (Na, B, Si, and Al) **as a function of time for LAWA44 glass at target pH = 8.5, 9.5, and 10.5 of 0.1 M NH_4Cl/NH_3 solution at RT, 40 °C, and 60 °C.** Error bars represent one standard deviation of triplicate measurements, where error bars are not visible they are smaller than the symbol size.

example, for 15 mins–8 h at pH 8.5, NLR_B increased by one order of magnitude from $(4.74 \pm 0.34) \times 10^{-4}$ g m^{-2} d^{-1} (RT) to $(3.04 \pm 0.55) \times 10^{-3}$ g m^{-2} d^{-1} (60 °C). The effect of increasing pH was less pronounced over the pH range 8.5–10.5; for example, over 15 mins–8 h at RT for both pH 8.5 and 9.5, NLR_B remained similar, being $(4.74 \pm 0.34) \times 10^{-4}$ g m^{-2} d^{-1} and $(1.79 \pm 0.47) \times 10^{-4}$ g m^{-2} d^{-1}, respectively.

Incongruent leaching in the low temperature, short-term EPA 1313 test suggests a dominant leaching mechanism that is different than the mechanism for standard dilute test conditions such as SPFT, which is aimed at ascertaining the 'forward rate' of dissolution as defined by the congruent dissolution of both network modifying and network forming elements[42,43]. During SPFT elemental release is measured once the experiment has reached a steady state (after some days/h) and once the network hydrolysis dominates over interdiffusion/ion exchange. Supplementary Fig. 13 shows the linear regression of $\log_{10}$ dissolution rates against the inverse of temperature (calculated according to the SPFT standard method)[43] for the data points collected for both early (R_0(B)) and later (R_l(B)) periods at various temperatures (RT, 40 °C and 60 °C) and pH (8.5, 9.5, and 10.5) conditions. Even though the dissolution under EPA 1313 test conditions is not in the forward rate regime, activation energy (E_a) can still provide insights into the rate-limiting step. The E_a values, calculated using linear fitting data analysis, are listed in Supplementary Table 15. The E_a for individual pH values at varying temperatures are listed for both the early and later time point trend and for the full 8 days. The activation energies for the buffered (TRIS and ammonia buffer) test ranged from 31-57 kJ mol^{-1}, notably lower than reported E_a values obtained using SPFT on LAWA44 glasses: 60 ± 7 kJ mol^{-7} and 71 kJ mol^{-1} [14] (calculated from NL_B). The lower values are indicative of ion exchange and interdiffusion processes dominating rather than the more energy-intensive hydrolysis process[44–48]. This is consistent with the observed incongruent leaching behaviour of Na observed with both TRIS and ammonium buffer systems and it must be concluded that the EPA 1313 test using these buffers, despite low temperatures, agitated conditions and short timescales, does not provide comparable data to tests designed to measure the forward rate for glass dissolution under dilute conditions, for example the SPFT or Microchannel Flow-Through (MCFT) test.

Disscussion

TRIS buffer at 0.1 M concentration was shown to be effective for use in EPA 1313 type tests up to pH 10.5 at room temperature but only up to pH 9.5 at elevated temperatures (40 °C and 60 °C), exhibiting a reduction in pH from the set value that was slight at 40 °C (from pH 10.5 to 10) but significant at 60 °C (from 10.5 to pH 9.0). The ammonium buffer was shown to be effective up to pH 10.5 at temperatures up to 60 °C. For both the buffered media, the normalized mass loss (NL_i) for Na, B, Si and Al increased with increasing temperature and decreased with increasing pH. In both buffers, NL_{Na} was higher than other elements at all experimental conditions indicating ion exchange processes outpaced network hydrolysis over these short timescales.

Despite similar trends and elemental releases being of the same order of magnitude, there were some differences in test response using the two different buffers that point to an influence of the buffer on the glass dissolution. TRIS buffer exhibited congruent B, Si, and Al release at low temperatures (RT, 40 °C) with pH 9.5 and 10.5, while incongruent leaching was observed at 60 °C likely due to the formation of surface alteration layers.

Table 1 | Dissolution rates of boron (NLR_B) in g m^{-2} d^{-1} as a function of temperature and pH at different time points for LAWA44 / TRIS-HNO_3 and ammonium buffered EPA 1313 tests

Timeframe	pH	Temperature/°C)	Normalised dissolution rate NLR_B (g m^{-2} d^{-1})			
			TRIS buffer	R^2	Ammonium buffer	R^2
15 min to 8 h data	8.5	RT	$(4.74 \pm 0.34) \times 10^{-4}$	0.97	$(3.25 \pm 0.64) \times 10^{-4}$	0.83
		40	$(4.92 \pm 0.46) \times 10^{-4}$	0.96	$(1.56 \pm 0.27) \times 10^{-3}$	0.87
		60	$(3.04 \pm 0.55) \times 10^{-3}$	0.85	$(6.44 \pm 1.14) \times 10^{-3}$	0.86
	9.5	RT	$(1.79 \pm 0.47) \times 10^{-4}$	0.73	$(3.42 \pm 0.12) \times 10^{-4}$	0.99
		40	$(5.60 \pm 0.56) \times 10^{-4}$	0.95	$(1.03 \pm 0.14) \times 10^{-3}$	0.91
		60	$(2.11 \pm 0.34) \times 10^{-3}$	0.88	$(4.61 \pm 0.82) \times 10^{-3}$	0.86
	10.5	RT	$(2.95 \pm 0.50) \times 10^{-4}$	0.87	$(4.36 \pm 1.13) \times 10^{-4}$	0.73
		40	$(6.00 \pm 1.33) \times 10^{-4}$	0.79	$(6.62 \pm 0.62) \times 10^{-4}$	0.96
		60	$(3.01 \pm 0.19) \times 10^{-3}$	0.98	$(2.48 \pm 0.43) \times 10^{-3}$	0.86
24 h to 96 h data	8.5	RT	$(6.62 \pm 0.60) \times 10^{-5}$	0.98	$(1.35 \pm 0.37) \times 10^{-4}$	0.80
		40	$(2.07 \pm 1.24) \times 10^{-4}$	0.99	$(2.38 \pm 0.90) \times 10^{-4}$	0.77
		60	$(7.98 \pm 1.08) \times 10^{-4}$	0.95	$(7.78 \pm 0.64) \times 10^{-4}$	0.98
	9.5	RT	$(4.34 \pm 0.41) \times 10^{-5}$	0.97	$(7.91 \pm 0.47) \times 10^{-5}$	0.99
		40	$(1.62 \pm 0.10) \times 10^{-4}$	0.94	$(3.49 \pm 0.34) \times 10^{-4}$	0.97
		60	$(4.48 \pm 0.28) \times 10^{-4}$	0.99	$(4.85 \pm 0.23) \times 10^{-4}$	0.99
	10.5	RT	$(7.31 \pm 0.48) \times 10^{-5}$	0.99	$(9.97 \pm 0.46) \times 10^{-5}$	1.00
		40	$(3.70 \pm 0.58) \times 10^{-4}$	0.93	$(3.50 \pm 0.50) \times 10^{-4}$	0.94
		60	$(6.60 \pm 0.48) \times 10^{-4}$	0.98	$(2.79 \pm 0.11) \times 10^{-4}$	1.00
15 min to 8 d data	8.5	RT	$(8.65 \pm 1.35) \times 10^{-5}$	0.79	$(1.43 \pm 0.27) \times 10^{-4}$	0.70
		40	$(2.30 \pm 0.24) \times 10^{-4}$	0.89	$(3.70 \pm 0.38) \times 10^{-4}$	0.89
		60	$(9.50 \pm 0.59) \times 10^{-4}$	0.96	$(9.72 \pm 1.29) \times 10^{-4}$	0.83
	9.5	RT	$(8.04 \pm 0.44) \times 10^{-5}$	0.97	$(7.19 \pm 0.66) \times 10^{-5}$	0.91
		40	$(1.72 \pm 0.12) \times 10^{-4}$	0.94	$(3.39 \pm 0.36) \times 10^{-4}$	0.89
		60	$(6.72 \pm 0.32) \times 10^{-4}$	0.98	$(6.75 \pm 1.09) \times 10^{-4}$	0.77
	10.5	RT	$(7.54 \pm 0.42) \times 10^{-5}$	0.97	$(8.48 \pm 1.30) \times 10^{-5}$	0.81
		40	$(2.54 \pm 0.29) \times 10^{-4}$	0.87	$(2.75 \pm 0.17) \times 10^{-4}$	0.96
		60	$(7.37 \pm 0.48) \times 10^{-4}$	0.95	$(4.05 \pm 0.54) \times 10^{-4}$	0.83

Ammonium buffer, however, showed an incongruent leaching throughout with evidence suggesting that ammonium ions can partake in ion exchange at the glass surface enhancing the release of network modifying cations and possibly to an indirect effect on other elements. Na release increased with increasing concentration of ammonia buffer and was elevated when compared to the same pH and temperature conditions with TRIS buffer.

The formation of a TRIS-boron complex was confirmed by ^{11}B NMR but there was no evidence that complexation affected the release of boron. There was no increase in the NL_B with increasing concentrations of TRIS from 0.02 M to 0.3 M as might be expected if TRIS were affecting boron release and NL_B was either comparable or slightly lower when compared to the same pH and temperature conditions with ammonia buffer. Finally, if the TRIS buffer were aiding the breaking of B-O bonds then incongruent release of boron might be expected; however, B, Si, and Al were released congruently at pH 9.5 and 10.5 both at RT and 40 °C. Previously, the effect of TRIS on the glass dissolution rate was studied by both Tournie et al. and Stone-Weiss et al. In the study by Tournie et al.[23], where a 5-component borosilicate glass was reacted at 80 °C and 20 m^{-1} for up to 3 h in a 0.05 M TRIS/HNO_3 system at pH 7.3, an increase by a factor of four in the reaction rate was observed for the 0.05 M TRIS/HNO_3 system compared to the DIW system. The increase in rate was attributed to a TRIS-boron complexation that increased the chemical potential between the boron in the glass and solution. In the study by Stone-Weiss et al.[22], where a $25Na_2O$–$25B_2O_3$–$50SiO_2$ glass (mol%) was reacted at 65 °C and 2.5 m^{-1} for 15–24 h in a 0.1 M TRIS/HNO_3 solution at pH 7, 8, and 9, no significant impact on the dissolution behaviour of the borosilicate glass was observed. In the present study, we have made similar observations as Stone-Weiss et al. Namely, though a TRIS-boron complex is observed in NMR measurements, no statistically significant increase in the glass dissolution rate was measured. Overall this study concludes that TRIS is a suitable buffer for use in EPA1313 type tests to give pH-dependent elemental release data over short timescales.

Experimental

Materials. The glass composition LAWA44 was supplied by Pacific Northwest National Laboratories (PNNL) (Table 2). The reagents used to make the two buffer solutions are tri(hydroxymethyl)aminomethane (TRIS) ($C_4H_{11}NO_3$) (≥99%, Fisher Chemicals), HNO_3 (65%, Fisher Chemicals), isopropanol (≥99.8%, Sigma Aldrich), ammonium hydroxide (NH_4OH) (28–30%, ACROS organic), and ammonium chloride (NH_4Cl) (99+%, Extra Pure, SLR, Fisher Chemical).

Methods

EPA 1313 is a dynamic leach test protocol[49], modified for use on glass[11], used to measure the elemental release of constituents from LAWA44 as a function of pH. In the present study, the standard method was further adapted to include the use of the two different metal-free buffer systems, TRIS and ammonium buffer, as an alternative to adjusting the pH by a one-time acid addition. LAWA44 glass was crushed and sieved to a particle size fraction of 75–150 μm. To remove any fines, the sieved glass sample was ultrasonically

Table 2 | Composition of LAWA44 glass in oxide wt%

Components	Oxide wt%
Al_2O_3	6.39
B_2O_3	9.56
CaO	2.21
Cr_2O_3	0.11
Fe_2O_3	7.44
K_2O	0.58
MgO	1.82
MoO_3	0.01
Na_2O	21.32
Re_2O_7	0.07
SO_3	0.11
SiO_2	41.19
TiO_2	2.10
ZnO	3.28
ZrO_2	3.00

washed with isopropanol at least ten times until a clear supernatant was obtained. The resultant glass sample was dried at 90 °C for 4–12 h.

To initiate the test, 10 mL of the buffering media was added to 1 g of the glass sample in centrifuge tubes (one for each time point). Tubes containing this mixture were then constantly tumbled end over end at 28 rpm for 8 days under set temperature conditions of 18 ± 1 °C, 40 ± 1 °C, and 60 ± 1 °C. All tests were run in duplicate. Post dissolution, the leachate was removed, filtered through 0.22-μm filters (Whatman), and cooled to room temperature for the pH measurement that was taken using a Mettler Toledo FP20; accuracy ±0.01.

For further elemental analysis, the leachate was acidified with 100 μL of nitric acid (69%), and concentrations were measured through inductively coupled plasma-optical emission spectroscopy (ICP-OES, Thermofisher iCAP-duo6300). Solution data are provided in Supplementary Tables 4 and 11.

The post-reaction glass powder was analysed using X-ray diffraction (Bruker D2 Phaser XRD with a CuKα X-ray source (λ = 1.54056 Å)) to identify any secondary precipitates. Fourier Transformed Infra-red (FT-IR) spectra were recorded using a Perkin Elmer Frontier in ATR mode in the frequency range 500–4000 cm^{-1}.

^{11}B NMR spectra were recorded for as-prepared solution 1:1 Tris/boron at 18 °C, 40 °C, and 60 °C in situ and all the aliquot (18 °C, 40 °C, and 60 °C test samples) at room temperature on a Bruker AVIII 400 MHz spectrometer operating at 128.40 MHz with 10% D_2O in H_2O solvent.

Normalised mass loss and dissolution rate calculation

From the elemental concentration data collected by ICP-OES analysis, the normalised mass loss was calculated using:

$$\mathbf{NL_i} = \frac{(C_i - C_{i,b})V}{f_i SA} \quad (1)$$

where NL_i is the normalised mass loss for element i, in g m^{-2}; C_i is the average concentration of i in solution in the duplicate tests, in mg L^{-1}; $C_{i,b}$ is the average concentration of i in the blank tests, in mg L^{-1}; f_i is the mass fraction of element i in the glass, SA is the total surface area of the exposed glass, in m^2; and V is the volume of leachant, in m^3. Glass SA was estimated using a geometric method, where particles are assumed to be perfect spheres with a diameter equal to the mean particle size.

In addition to the NL_i, calculated from duplicate sacrificial vessels normalized leach rates (NLR_i) were also calculated. Rates were calculated from the gradient of the dissolution data over the time periods 15 min to 8 h; 1 d to 4 d; and 15 min to 8 d.

The linear fit of NL_i (measured between 15 min and 8 h, 24–96 h and 15 min–192 h) against time was performed using Origin 2018 software to determine the rates (early and later stages) from the slope values. Rate calculations were performed across all temperature and pH conditions. Further, to calculate the activation energy (E_a), the slope obtained from the plot of log(rate) vs 1/temperature (in kelvin) was used in accordance with the Arrhenius equation $r = A\exp(\frac{-E_a}{RT})$. This slope value was then multiplied by the gas constant (8.314 J mol^{-1} K^{-1}] and a factor of 2.303, and subsequently converted into kilojoules per mole (kJ mol^{-1}). The resulting activation energy values are summarized in Supplementary Table 15.

Solution preparation

To understand the impact of the buffer concentration on glass dissolution, 0.02 M, 0.05 M, 0.1 M, and 0.3 M solutions of TRIS and ammonium buffers were prepared in ultra-high quality ASTM Type 1 water (resistivity 18.2 MΩ cm^{-1})[30] obtained from a Millipore Direct-Q (U.V.) 3 water purification system.

The required amount of 1 M nitric acid was gradually added to this solution with constant stirring until the desired pH was obtained. Similarly, for the preparation of ammonium buffer, the required mass of ammonium chloride was dissolved in Type 1 water, and a desired pH was achieved by gradually adding 5 M ammonia with constant stirring.

Data availability

The data that support the findings of this study are available from the corresponding author upon reasonable request.

Received: 20 June 2024; Accepted: 1 January 2025;
Published online: 15 January 2025

References

1. ASTM C1285-21. *Standard Test Methods for Determining Chemical Durability of Nuclear, Hazardous, and Mixed Waste Glasses and Multiphase Glass Ceramics: The Product Consistency Test (PCT)* (ASTM International, West Conshohocken, 2021).
2. ASTM C1663-18. *Standard Test Method for Measuring Waste Glass or Glass Ceramic Durability by Vapor Hydration Test* (ASTM International, West Conshohocken, 2024).
3. ASTM C1662-18. *Standard Practice for Measurement of the Glass Dissolution Rate Using the Single-Pass Flow-Through Test Method* (ASTM International, West Conshohocken, 2018).
4. Hopf, J. et al. Toward an understanding of surface layer formation, growth, and transformation at the glass–fluid interface. *Geochim. Cosmochim. Acta* **229**, 65–84 (2018).
5. Thorpe, C. L. et al. Forty years of durability assessment of nuclear waste glass by standard methods. *npj Mater. Degrad.* **5**, 61 (2021).
6. Muller, I. S. et al. *Baseline LAW Glass Formulation Testing*, VSL-03R3460-1, Rev. *0*. (No. ORP-59016 Rev. 0) (Hanford Site (HNF), Richland, 2015).
7. Pierce, E. M. et al. *Waste Form Release Data Package for the 2005 Integrated Disposal Facility Performance Assessment (No. PNNL-14805)* (Pacific Northwest National Lab. (PNNL), Richland, 2004).
8. DOE. *Contract DE-AC27–01RV14136 (as amended)* (U.S. Department of Energy, Office of River Protection, Richland, 2001).
9. Marcial, J. et al. Evaluating an EPA leaching test (Method 1313) to relate the long-term performance of nuclear waste glasses and ancient glasses -21243. In *Waste Management Conference Proceeding Phoenix, AZ* (2021 Waste Management Symposia, 2021).
10. Marcial, J. et al. *Chemical durability assessment of enhanced low-activity waste glasses through EPA method 1313* (No. PNNL-32663) (Pacific Northwest National Laboratory (PNNL), Richland, 2023).

11. Thorpe, C. L. et al. Evaluation of novel leaching assessment for nuclear waste glasses. In *WM2018 Conference* 18–22 (WM, Arizona, 2018).
12. Ross, W. A., Strachan, D. M., Turcotte, R. P. & Westsik, Jr. J. H. *Materials Characterization Center Workshop on Leaching of Radioactive Waste Forms. Summary Report (No. PNL-3318) (*Battelle Pacific Northwest Labs., Richland, 1980).
13. Barkatt, A. et al. Mechanisms of defense waste glass dissolution. *Nucl. Technol.* **73**, 140–164 (1986).
14. Vienna, J. D., Neeway, J. J., Ryan, J. V. & Kerisit, S. N. Impacts of glass composition, pH, and temperature on glass forward dissolution rate. *npj Mater. Degrad.* **2**, 22 (2018).
15. DOE. Hanford Site RCRA Groundwater Monitoring Report for 2023, DOE/RL-2023-53. https://www.hanford.gov/files.cfm/DOE-RL-2023-53_R0_Combined_clean.pdf (2023).
16. Backhouse, D. J. et al. Corrosion of the international simple glass under acidic to hyperalkaline conditions. *npj Mater. Degrad.* **2**, 1–10 (2018).
17. Jollivet, P., Gin, S. & Schumacher, S. Forward dissolution rate of silicate glasses of nuclear interest in clay-equilibrated groundwater. *Chem. Geol.* **330**, 207–217 (2012).
18. Ferguson, W. J. et al. Hydrogen ion buffers for biological research. *Anal. Biochem.* **104**, 300–310 (1980).
19. Ferreira, C. M., Pinto, I. S., Soares, E. V. & Soares, H. M. (Un)suitability of the use of pH buffers in biological, biochemical and environmental studies and their interaction with metal ions-a review. *RSC Adv.* **5**, 30989–31003 (2015).
20. Gomori, G. Buffers in the range of pH 6.5 to 9.6. *Proc. Soc. Exp. Biol. Med.* **62**, 33–34 (1946).
21. Icenhower, J. P. et al. Experimentally determined dissolution kinetics of Na-rich borosilicate glass at far from equilibrium conditions: Implications for transition state theory. *Geochim. Cosmochim. Acta* **72**, 2767–2788 (2008).
22. Stone-Weiss, N., Smith, N. J., Youngman, R. E., Pierce, E. M. & Goel, A. Dissolution kinetics of a sodium borosilicate glass in tris buffer solutions: impact of tris concentration and acid (HCl/HNO_3) identity. *Phys. Chem. Chem. Phys.* **23**, 16165–16179 (2021).
23. Tournié, A. et al. Impact of boron complexation by tris buffer on the initial dissolution rate of borosilicate glasses. *J. Colloid Interface Sci.* **400**, 161–167 (2013).
24. Çallı, M. & Pehlivan, E. Effects of adding boron compounds to glycol based grinding aids on cement compressive strengths performance. *Open J. Civ. Eng.* **09**, 35–45 (2019).
25. Beynon, R. & Easterby, J. *Buffer Solutions* (CRC Press, 2004).
26. Petrucci, R. H. & Wismer, R. K. *General chemistry with qualitative analysis* (Macmillan, 1987).
27. WANG, L. et al. Chemical stability of simulated waste forms $Zr_{1-x}Nd_xSiO_{4-x/2}$: influence of temperature, pH and their combined effects. *J. Rare Earths* **35**, 709–715 (2017).
28. Mazer, J. J. & Walther, J. V. Dissolution kinetics of silica glass as a function of pH between 40 and 85 °C. *J. Non Cryst. Solids* **170**, 32–45 (1994).
29. Fox, K., Edwards, T., & Riley, W. *Chemical Compo*sition Measurements of LAWA44 Glass Samples. SRNL-STI--2016-00617 (IAEA, Aiken, 2016).
30. ASTM D1193-99e1. *Standard Specification for Reagent Water* https://www.astm.org/d1193-99e01.html (2017).
31. Stoll, V. S. & Blanchard, J. S. Buffers: principles and practice. *Methods Enzymol.* **463**, 43–56 (2009).
32. Majérus, O., Gérardin, T., Manolescu, G., Barboux, P. & Caurant, D. Effect of aqueous $Mg^{2+}$and Ca^{2+} cations on the dissolution kinetics and alteration layer of sodium borosilicate glasses at neutral pH buffered with Tris/HCl. *Phys. Chem. Glas. Eur. J. Glas. Sci. Technol. Part B* **55**, 261–273 (2014).
33. Nava-Farias, L. et al. Applying laboratory methods for durability assessment of vitrified material to archaeological samples. *npj Mater. Degrad.* **5**, 1–15 (2021).
34. Pierce, E. M., Rodriguez, E. A., Calligan, L. J., Shaw, W. J. & Pete McGrail, B. An experimental study of the dissolution rates of simulated aluminoborosilicate waste glasses as a function of pH and temperature under dilute conditions. *Appl. Geochem.* **23**, 2559–2573 (2008).
35. Chappex, T. & Scrivener, K. L. The effect of aluminum in solution on the dissolution of amorphous silica and its relation to cementitious systems. *J. Am. Ceram. Soc.* **96**, 592–597 (2013).
36. Yanagisawa, N., Fujimoto, K., Nakashima, S., Kurata, Y. & Sanada, N. Micro FT-IR study of the hydration-layer during dissolution of silica glass. *Geochim. Cosmochim. Acta* **61**, 1165–1170 (1997).
37. Sidey, V. On the effective ionic radii for ammonium. *Acta Crystallogr. B.* **72**, 626–633 (2016).
38. Shannon, R. D. Revised effective ionic radii and systematic studies of interatomic distances in halides and chalcogenides. *Acta Cryst. A* **32**, 751–767 (1976).
39. Yuan, J., Yang, J., Ma, H. & Liu, C. Crystal structural transformation and kinetics of NH4+/Na+ ion-exchange in analcime. *Micropor. Mesopor. Mat.* **222**, 202–208 (2016).
40. Hankins, N. P., Pliankarom, S. & Hilal, N. An equilibrium ion-exchange study on the removal of NH4+ ion from aqueous effluent using clinoptilolite. *Sep. Sci. Technol.* **39**, 3639–3663 (2005).
41. Sugiura, Y., Makita, Y. & Horie, M. Ammonium-to-sodium ion-exchange process at the interlayer of octacalcium phosphate. *RSC adv.* **11**, 39503–39507 (2021).
42. Elia, A., Ferrand, K. & Lemmens, K. Determination of the forward dissolution rate for international simple glass in alkaline solutions. *MRS Adv.* **2**, 661–667 (2017).
43. ASTM. *C1662-18 Standard Practice for Measurement of the Glass Dissolution Rate Using the Single-Pass Flow-Through Test Method* (ASTM International, 2024).
44. Ojovan, M. I., Pankov, A. & Lee, W. E. The ion exchange phase in corrosion of nuclear waste glasses. *J. Nucl. Mater.* **358**, 57–68 (2006).
45. Ojovan, M. I., Lee, W. E. & Hand, R. J. Role of ion exchange in the corrosion of nuclear waste glasses. *Mater. Res. Soc. Symp. Proc.* **932**, 393–400 (2006).
46. McGrail, B. P. et al. *Low-Activity Waste Glass Studies: FY2000 Summary Report (No. PNNL-13381)* (Pacific Northwest National Lab. (PNNL), Richland, 2000).
47. Neeway, J. J., Rieke, P. C., Parruzot, B. P., Ryan, J. V. & Asmussen, R. M. The dissolution behavior of borosilicate glasses in far-from equilibrium conditions. *Geochim. Cosmochim. Acta* **226**, 132–148 (2018).
48. Ojovan, M. I. et al. Corrosion mechanisms of low level vitrified radioactive waste in a loamy soil. *Mater. Res. Soc. Symp. Proc.* **824**, CC5.8.1–CC5.8.6 (2004).
49. E. P. A. Method 1313, *Liquid–Solid Partitioning as a Function of Extract pH Using a Parallel Batch Extraction Procedure. SW-846 Update VII, Revision 1* (EPA, Washington, DC, 2019).

Acknowledgements

The authors gratefully acknowledge the financial support provided by the U.S. Department of Energy Waste Treatment and Immobilization Plant Project, under the auspices of Project GLAD (Glass Leachability for Disposal Assessment). Albert Kruger, Office of River Protection, served as programme manager. This research also utilised the HADES/MIDAS and PLEIADES National Nuclear User Facilities, established with financial support from EPSRC and BEIS, under grant numbers EP/T011424/1 and EP/V035215/1. C.L.C. and C.L.T. wish to acknowledge the Engineering and Physical Science Research Council (EPSRC) for fellowship funding under grant awards EP/N017374/1 and EP/S012400/1, respectively. C.L.T. wishes to acknowledge the support of the Royal Society under the Dorothy Hodgkin Fellowship scheme.

Author contributions

R.R. conducted all experimental work with assistance from C.L.T., C.L.C., S.A.W. and R.J.H., J.J.N., C.I.P., A.A.K., D.S.K. and J.M. contributed

experience and expertise regarding the EPA 1313 test and glass dissolution testing. All authors contributed to the detailed revision of the manuscript, editing, critical review and approved the final document.

Competing interests
The authors declare no competing interests.

Additional information
Supplementary information The online version contains supplementary material available at https://doi.org/10.1038/s41529-025-00552-3.

Correspondence and requests for materials should be addressed to Clare L. Thorpe.